PhD in Information Technology and Electrical Engineering

Università degli Studi di Napoli Federico II

Training and Research Activities Report First Year

XXIX Cycle

PhD Student:
Mahdi Momeni Kelageri

Tutor:
Vincenzo Lippiello

February 22, 2015

Preface

I believe that in the life we are results of each passed moment we had lived in and that our mentality is created and formed based on difficulties we have to deal with. The more the difficulties we had and succeeded to overcome, the more the ability we will have to deal with other difficulties that may appear in the future even if they are not belonging to the same sort of difficulties we had experienced before. We just gain the logic of thinking how to avoid difficulties. In my opinion, the only important point is to have the ability to free our mind from any constraints that may set any limits to our way of thinking about those problem issues considered. In this view, I would like to think of every moment in my life, and every person who had a positive signature kept in my mentality and my life. In this regard, first and foremost, I express my deepest and warmest gratitudes to my parents. If it was not for their kind support and patience, I have no idea where I would be now. Then, I am deeply indebted to Professor Bruno Siciliano, Professor Vincenzo Lippiello and Dr. Fabio Ruggiero for their helpful guidance, great care, valuable advices, continuous and indispensable assistance and opening new windows to different aspects of science and technology to me. I leanred a lot more than I could even imagine during my first year presence in PRISMA lab and the project I had taken under supervision of them. Furthermore, I also heartly thank all the other PIRSMA lab members for all their supports in the past year.

Mahdi Momeni
February 22, 2015

Contents

List of Figures

Chapter 1

Information

1.1 Name Surname, MS title – University

- **First Name:** Mahdi
- **Last Name:** Momeni Kelageri
- **M.Sc. Title:** Electrical and Electronic Engineering
- **University:** Pusan National University, Pusan, South Korea

1.2 Cycle – Department

- **PhD Cycle:** XXIX
- **Department:** Information Technology and Electrical Engineering

1.3 Fellowship Type

- **Fellowship:** CREATE

1.4 Tutor

- **Tutor:** Prof. Vincenzo Lippiello

Chapter 2

Study and Training Activities

For detailed tabular description of the study and training activities, please refer to Appendix A.

2.1 Courses

- Robot Control
  - Tutor: Prof. B. Siciliano
  - No. of Credits: 9 CFU
  - Certificate: No
- Multivariable Control
  - Tutor: Prof. G. Celentano
  - No. of Credits: 6 CFU
  - Certificate: No
- The Entrepreneurial Analysis of Engineering Research Projects
  - Tutor: Prof. L. Iandoli
  - No. of Credits: 3 CFU
  - Certificate: No
- Three core issues for the Internet: things, security and economics (2 CFU)
  - Tutor: Prof. H. Schulzrinne
  - No. of Credits: 2 CFU
  - Certificate: Yes

2.2 Seminars

- Half day Workshop on "*Efficient service distribution in next generation cloud networks*"
  - Organizer: Prof. A. Tulino
  - No. of hours: 4

  - Certificate: Yes

- "*Developmental Robotics: From Babies to Robots*"
  - Presenter: Prof. A. Cangelosi
  - No. of hours: 1
  - Certificate: Yes

- "*Towards agile flight of vision-controlled micro flying robots: from frame-based to event-based vision*"
  - Presenter: Prof. D. Scaramuzza
  - No. of hours: 1
  - Certificate: Yes

Chapter 3

Research Activities

In this chapter, two different research topics pursued during the last year are explained:

- March 2014 - September 2014: *Robotic Machining*
- September 2014 - March 2015: *Controllabiliy of Underactuated and Non-Affine Nonlinear Systems*

3.1 Robotic Machining

External forces applied to the end-effector of an industrial robot will deform the manipulator due to it's low stiffness. This, in turn, will cause some positioning error. As a result, the current end-effector's position should be modified and compensated for the error due to the robot's deformation. To this end, it's necessary to identify and model the robot's stiffness in order to use it in robot control loop.

3.1.1 Robot Deformation Modeling

The relationship between the vector of the compliant displacements $\mathbf{\Delta X} = [\Delta x\ \Delta y\ \Delta z\ \Delta\varphi\ \Delta\psi\ \Delta\theta]^T$ and external wrench $\mathbf{W} = [F_x\ F_y\ F_z\ T_x\ T_y\ T_z]^T$ in reference frame $o - xyz$ can be written as:

$$\mathbf{W} = \mathbf{K}\ \mathbf{\Delta X}, \tag{3.1}$$

where $\mathbf{K}_{6\times6}$ is called the Cartesian stiffness matrix.It is worth noting that $\mathbf{K}$ depends on the choice of the reference frame in which $\mathbf{\Delta X}$ and $\mathbf{W}$ are defined. As a result, if one defines the new reference frame $o' - x'y'z'$, Eq. 3.1 will change to $\mathbf{W'} = \mathbf{K'}\ \mathbf{\Delta X'}$ where in general $\mathbf{K} \neq \mathbf{K'}$. However, $\mathbf{W'}$ and $\mathbf{\Delta X'}$ can be related to $\mathbf{W}$ and $\mathbf{\Delta X}$ using the following equations:

$$\begin{cases} \mathbf{W'} = \mathbf{A}\ \mathbf{W} \\ \mathbf{\Delta X'} = \mathbf{a}\ \mathbf{\Delta X} \end{cases}, \tag{3.2}$$

where:

$$\begin{cases} \mathbf{A} = \begin{bmatrix} {}^{o'}\mathbf{R}_o & \mathbf{0}_{3\times3} \\ {}^{o'}\mathbf{P}_o \times {}^{o'}\mathbf{R}_o & {}^{o'}\mathbf{R}_o \end{bmatrix} \\ \mathbf{a} = \begin{bmatrix} {}^{o'}\mathbf{R}_o & \mathbf{0}_{3\times3} \\ \mathbf{0}_{3\times3} & {}^{o'}\mathbf{R}_o \end{bmatrix} \end{cases}, \tag{3.3}$$

where ${}^{o'}\mathbf{R}_o$ and ${}^{o'}\mathbf{P}_o$ are the rotation and position matrices representing the orientation of the frame $o - xyz$ w.r.t the frame $o' - x'y'z'$, respectively.

Using Eq. 3.2, it is also possible to find out the external wrench applied to each component of the industrial manipulator. In other words, expanding Eq. 3.2, one can easily show that for each component of the robot the following equation holds:

$$\begin{cases} {}^{j}\mathbf{F}_j = {}^{j}\mathbf{R}_i \ {}^{i}\mathbf{F}_i \\ {}^{j}\mathbf{T}_j = {}^{j}\mathbf{R}_i \ ({}^{i}\mathbf{F}_i \times {}^{i}\mathbf{P}_j + {}^{i}\mathbf{T}_i) \end{cases}, \tag{3.4}$$

where ${}^{i}\mathbf{P}_j$ and ${}^{j}\mathbf{R}_i$ are the position of the origin of coordinate frame j w.r.t frame i and rotation of coordinate frame i w.r.t frame j, respectively. Consequently, by using equations 3.1 and 3.4, it is then possible to measure the compliant displacement of the origins of the coordinate systems attached to each component. Having found the deviation of the origins of all 6 coordinate frames due to the external wrench, it is possible to calculate the new homogeneous transformation matrices corresponding to each component, considering the change in joint variables due to the external wrench.

To measure the total compliant displacement, it is possible to use the forward kinematics:

$${}^{0}\mathbf{T}'_6 = {}^{0}\mathbf{T}'_1 \times {}^{1}\mathbf{T}'_2 \times {}^{2}\mathbf{T}'_3 \times {}^{3}\mathbf{T}'_4 \times {}^{4}\mathbf{T}'_5 \times {}^{5}\mathbf{T}'_6, \tag{3.5}$$

where ${}^{i-1}\mathbf{T}'_i, i = 1, ..., 6$ are the transformation matrices corresponding to the new joint variables. As a result, the total compliant displacement of the robot end-effector can be calculated by comparing the ${}^{0}\mathbf{T}_6$ and ${}^{0}\mathbf{T}'_6$, where ${}^{0}\mathbf{T}_6$ is the transformation matrix before the external forces are exerted. This means that $\mathbf{\Delta P}$ and $\mathbf{\Delta R}$ represent the total compliant displacement of the robot end-effector where:

$$\begin{cases} \mathbf{\Delta P} = {}^{0}\mathbf{P}_6 - {}^{0}\mathbf{P}'_6 \\ \mathbf{\Delta R} = {}^{0}\mathbf{R}_6^{-1} {}^{0}\mathbf{R}'_6 \end{cases}. \tag{3.6}$$

It is worth noting that, if desired, the deflection of the origin of each joint can be calculated by comparing the initial unloaded transformation matrix with the loaded transformation matrix for the corresponding serial kinematic chain. In other word, the generalized form of Eq. 3.6 can be used to calculate the deflection of each joint due to the external wrench:

$$\begin{cases} \mathbf{\Delta P} = {}^{0}\mathbf{P}_i - {}^{0}\mathbf{P}'_i \\ \mathbf{\Delta R} = {}^{0}\mathbf{R}_i^{-1} {}^{0}\mathbf{R}'_i \end{cases}, \tag{3.7}$$

where i stands for the desired joint. Equation 3.7 can also be used to find out how accurate the deflection of each joint is calculated by comparing it with the measured frames under load (compare Section **??**).

3.1.2 Mathematical Formulation

The evaluation of stiffness matrix $\mathbf{K}$ in Eq. 3.1 can be carried out using a least square approach, provided that the full wrench vector and the full pose displacement, i.e. displacement in position and orientation, can be measured in the same coordinate frame.
Considering the frame $o - xyz$, the external wrench and the corresponding deformation in this frame can be expressed as:

$$\begin{cases} \mathbf{W} = [F_x \ F_y \ F_z \ T_x \ T_y \ T_z]^T \\ \mathbf{\Delta X} = [\Delta x \ \Delta y \ \Delta z \ \Delta\varphi \ \Delta\psi \ \Delta\theta]^T \end{cases}. \tag{3.8}$$

The fitting error is expressed as:

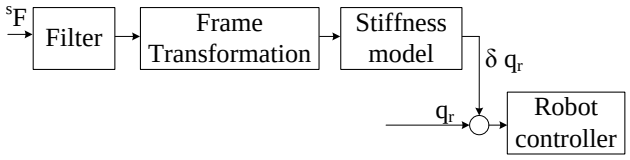

Figure 3.1: Real-Time deformation compensation block diagram; ${}^{s}F$, δq_r and q_r represent the external force, deformation in reference, and reference joint angles, respectively.

$$\mathbf{e} = \sum_{i=1}^{N} \mathbf{e}_i^T \, \mathbf{e}_i = \sum_{i=1}^{N} \mathbf{W}_i \, \mathbf{W}_i^T - (\sum_{i=1}^{N} \boldsymbol{\Delta}\mathbf{X}_i \, \mathbf{W}_i^T)^T \, \mathbf{K}. \tag{3.9}$$

Equation 3.1 can be re-written in the following form:

$$\mathbf{W}^T = \boldsymbol{\Delta}\mathbf{X}^T \, \mathbf{K}^T. \tag{3.10}$$

The objective is to minimize:

$$S(\mathbf{K}) = \|\mathbf{W}^T - \boldsymbol{\Delta}\mathbf{X}^T \, \mathbf{K}^T\|^2. \tag{3.11}$$

Equation 3.11 is equivalent to:

$$\begin{aligned} S(\mathbf{K}) &= (\mathbf{W}^T - \boldsymbol{\Delta}\mathbf{X}^T \, \mathbf{K}^T)^T \, (\mathbf{W}^T - \boldsymbol{\Delta}\mathbf{X}^T \, \mathbf{K}^T) \\ &= \mathbf{W}\mathbf{W}^T - \mathbf{W}\boldsymbol{\Delta}\mathbf{X}^T\mathbf{K}^T - \mathbf{K}\boldsymbol{\Delta}\mathbf{X}\mathbf{W}^T + \mathbf{K}\boldsymbol{\Delta}\mathbf{X}\boldsymbol{\Delta}\mathbf{X}^T\mathbf{K}^T. \end{aligned} \tag{3.12}$$

Differentiating the resulting equation with respect to $\mathbf{K}$ and equating to zero gives:

$$-2\boldsymbol{\Delta}\mathbf{X}\mathbf{W}^T + 2\boldsymbol{\Delta}\mathbf{X}\boldsymbol{\Delta}\mathbf{X}^T\mathbf{K}^T = 0, \tag{3.13}$$

which gives:

$$\Rightarrow \mathbf{K}^T = (\boldsymbol{\Delta}\mathbf{X}\boldsymbol{\Delta}\mathbf{X}^T)^{-1}\boldsymbol{\Delta}\mathbf{X}\mathbf{W}^T. \tag{3.14}$$

Considering a set of N measurements, the least square solution of the Cartesian stiffness matrix $\hat{\mathbf{K}}$ is:

$$\hat{\mathbf{K}}^T = (\sum_{i=1}^{N} \boldsymbol{\Delta}\mathbf{X}_i \, \boldsymbol{\Delta}\mathbf{X}_i^T)^{-1} \, (\sum_{i=1}^{N} \boldsymbol{\Delta}\mathbf{X}_i \, \mathbf{W}_i^T). \tag{3.15}$$

Based on this formulation stiffness is identified from experimental data records.

3.1.3 Deformation Compensation

Figure 3.1 shows the block diagram of the real-time deformation compensation implemented in TwinCAT [1] for a KR 125 industrial manipulator of series 2000. The measurement noise has to be filtered out from force sensor data. Besides, the coordinate frame assigned to the force sensor is different from that of the robot base. As a result, the force sensor data is transformed to the robot base frame. On the other hand, in order to only deal with the external forces which are exerted to the end-effector due to the machining process, the weight of the force sensor, the fixture and the work piece are compensated. The deformation caused by machining forces is calculated in real-time using the model which is already developed, and the joint references trajectory is recalculated by the robot controller. Consequently, the end-effector pose is modified.

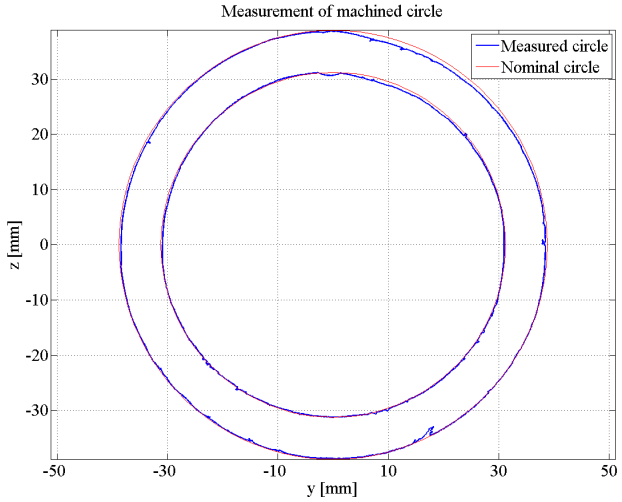

(a)

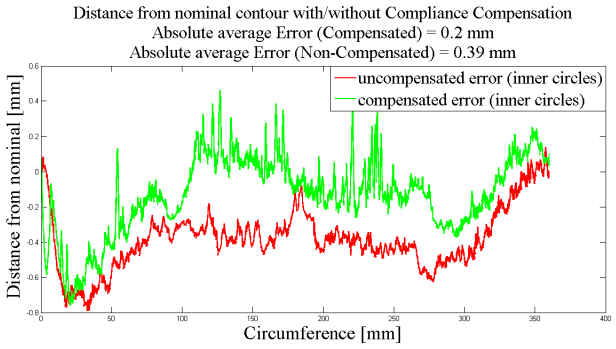

(b)

Figure 3.2: Experimental results a) machined circle and b) point-to-point error

3.1.4 Experimental Validation

In order to asses the effectiveness of the proposed deformation compensation method, milling tests on a steel block have been conducted. To this end, a Chopper 3300 spindle from Alfred Jaeger is used together with an $8mm$ endmill tool with four teeth from Hoffman Group. The purpose is to mill a circle of radius $35mm$. The results of the experiments are shown in figures 3.2a and 3.2b.

3.1.5 Achievments and Contributions

In this contribution, a new stiffness model with 36 degrees of freedom and nonlinear descriptions have been presented together with a new identification method which let us find the nondiagonal stiffness matrix $K_{6\times6}$. Validation of the model shows a reduction of the error due to the compliance by about 50% for all measurements. This fact can be seen in Fig.3.2a and 3.2b in which the machining error is reduced about 50%.

3.2 Nonprehensile Manipulation

Manipulation by grasping may be restrictive in some applications and it happens that manipulation of objects without grasping them like pushing, flipping, throwing and etc is required. One way to

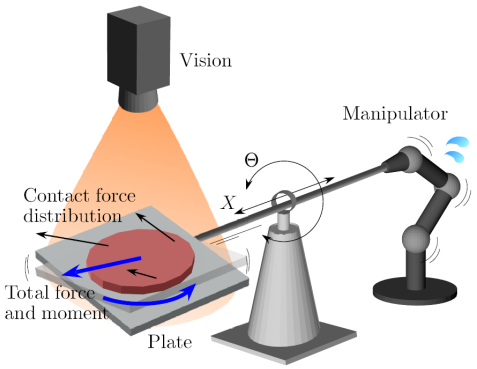

Figure 3.3: Hyper plate system with two active DOFs of X and θ

manipulate objects without grasping is through vibration. More specifically, it is desired to control the orientation and position of an object on top of a vibrating plate.

3.2.1 Objective

Figure 3.3 shows a dexterous hyper plate with a high-speed vision system. It is shown that with only 2 DOFs in plate's movement, it is possible to create a 3 DOF movement for the deformable object on top of it [2]. In particular, by translating the peel along and around x-axis it would be possible to move the object along x- and y- axes and around z-axis. The motion equations of such system are as following:

$$\begin{cases} m_B{}^m\ddot{x}_B = -m_B\ddot{X} - \frac{{}^m\dot{x}_B}{|{}^m\dot{x}_B|}\mu_k m_B g \\ m_B{}^m\ddot{y}_B = -m_B g sin(\theta) - \frac{{}^m\dot{y}_B}{|{}^m\dot{y}_B|}\mu_k m_B (gcos(\theta) + {}^m y_B\ddot{\theta} \\ n = -\frac{{}^m\dot{x}_B}{|{}^m\dot{x}_B|}\mu_k I_x({}^m\theta_B)\ddot{\theta} \end{cases}, \tag{3.16}$$

where:

$$I_x({}^m\theta_B) \triangleq \int_{m_B} ({}^m y_r - {}^m y_B)^2 dm, \tag{3.17}$$

corresponds to the moment of inertia around the axis that passes through the center of mass of the object and runs parallel with the x_m-axis, where the orientation of the object is given by ${}^m\theta_B$.

The goal in the above mentioned manipulation is to control the position and orientation of the deformable object through a vibrating plate. The control inputs to are:

$$\begin{cases} X(t) = \alpha sin(\omega\pi t) \\ \theta(t) = \beta sin(\omega\pi t) \end{cases}, \tag{3.18}$$

where α, β and ω are constants.

3.2.2 Results

In this part, the control inputs in Eq. 3.18 will be applied to the system and the outputs are represented.

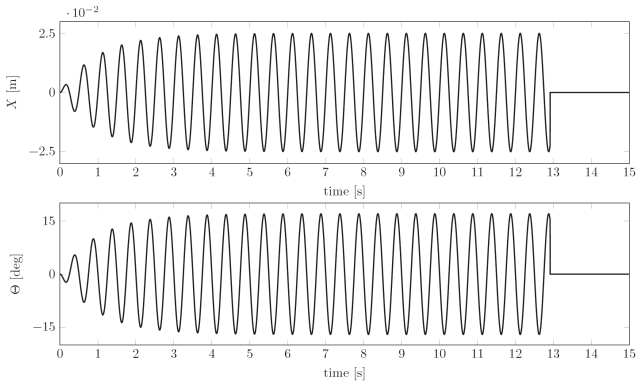

(a)

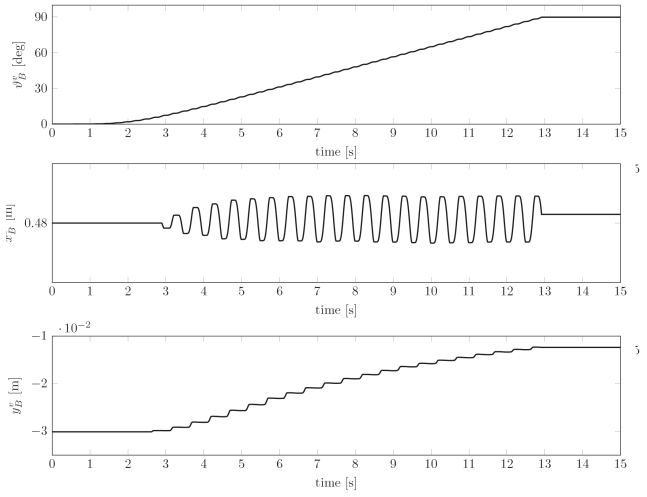

(b)

Figure 3.4: Simulation results a) input control signals and b) outputs

Orientation control

The following control input is applied to the system:

$$\begin{cases} X(t) = 0.025sin(4\pi t)\xi(t) \\ \theta(t) = -15sin(4\pi t)\xi(t) \end{cases}, \tag{3.19}$$

where $\xi(t) = 1 - \exp^{\frac{-t}{\tau}}$ is a damping factor of the initial signal and $\tau = 1$.

The goal is to change the rotatation of the object from 0° to 90°. Figure 3.4a and 3.4b show the input control signals and the outputs, respectively.

Position control along x-axis

The following control input is applied to the system:

$$\begin{cases} X(t) = (\frac{e_x}{|e_x|})(0.015 + 0.3|e_x|)(0.51 - 0.5cos(2\omega t) - 0.1cos(4\omega t))\xi(t) \\ \theta(t) = 0 \end{cases}. \tag{3.20}$$

The goal is to translate the object from initial position $x_B = 0.48m$ to $x_B = 0.54m$. Figure 3.5a and 3.5b show the input control signals and the outputs, respectively.

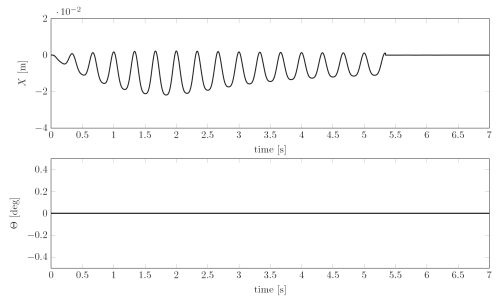

(a)

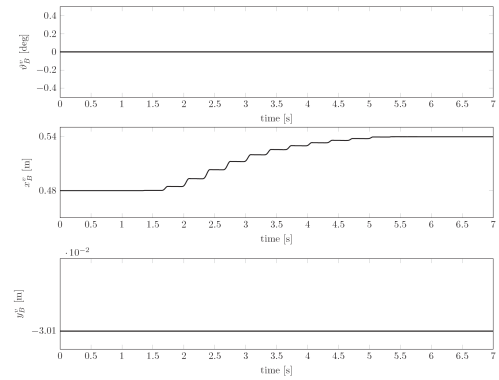

(b)

Figure 3.5: Simulation results a) input control signals and b) outputs

Position control along y-axis

The following control input is applied to the system:

$$\begin{cases} X(t) = 0 \\ \theta(t) = (\frac{e_y}{|e_y|})(20 + 200|e_y|)(\frac{1-cos(6\pi t)}{2})\xi(t) \end{cases} . \tag{3.21}$$

The goal is to translate the object from initial position $y_B = -0.03m$ to $y_B = 0.0m$. Figure 3.6a and 3.6b show the input control signals and the outputs, respectively.

3.2.3 Future Works

In the current control approach, to move the object to a desired position and orientation it's necessary to first control and adjust it's orientation and then, control it's position (2 steps control approach). The future work will include controlling the position and orientation of the object simultaneously. To this end, the controllability of the system has to be analyzed.

Problem Statement

The current mechanical system is an underactuated system which is non-affine in control system.

A nonlinear system in the following format is called non-affine in the control input or highly nonlinear system:

$$\dot{x} = f(x, u, t). \tag{3.22}$$

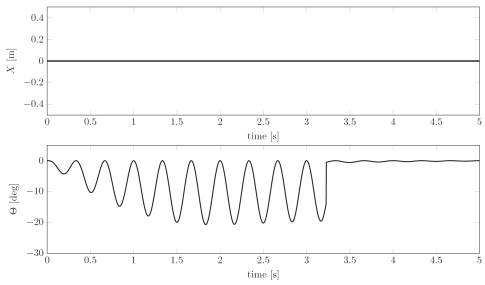

(a)

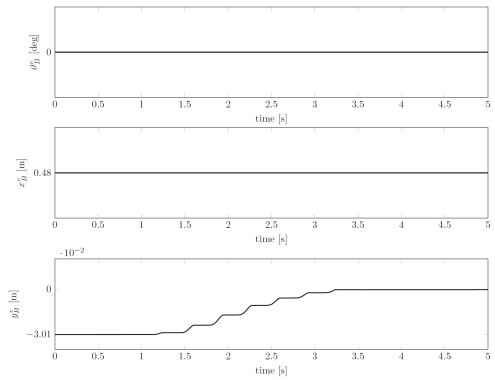

(b)

Figure 3.6: Simulation results a) input control signals and b) outputs

An underactuated nonlinear system is a system with less control input than the configuration variables (degree of freedoms). Mathematically speaking, the nonlinear system:

$$\ddot{q} = f(q, \dot{q}, u, t), \tag{3.23}$$

where:

- $q \in \mathbb{R}^n$ is configuration variable.
- $u \in \mathbb{R}^m$ is control input.
- t is time.

is underactuated if:

$$m < n$$

To my best knowledge, there is no rigirous approach to analyze the controllability of non-affine underactuated nonlinear systems. The only solution might be to find a coordinate transformation so that the non-affine nonlinear system is trasformed into an affine one[1]. Then, using *Lie Brackets* approach it is possible to analyze the controllability of the system. The future works, therefore, will be on finding a proper coordinate transfomation so that we are able to analyze the controllability of the system and thus, design a controller to control the position and orientation of the object simultaneously.

[1]the system in $\dot{x} = f(x) + g(x)u$ form is called affine in the control input

3.3 Research Products

- U. Schneider, M. Momeni-K, M. Ansaloni and A. Verl, "*Stiffness Modeling of Industrial Robots for Deformation Compensation in Machining*", IEEE/RSJ International Conference on Intelligent Robots and Systems (IROS), Chicago, Illinois, US; 09/2014

Appendix A

Credits

Student: Mahdi Momeni Kelageri Tutor: Vincenzo Lippiello Cycle XXIX
mahdi.momenikelageri@unina.it vincenzo.lippiello@unina.it

	Credits year 1							Credits year 2							Credits year 3								
	Estimated	1 bimonth	2 bimonth	3 bimonth	4 bimonth	5 bimonth	6 bimonth	Summary	Estimated	1 bimonth	2 bimonth	3 bimonth	4 bimonth	5 bimonth	6 bimonth	Summary	Estimated	1 bimonth	2 bimonth	3 bimonth	4 bimonth	5 bimonth	6 bimonth	Summary	Total	Check
Modules	18				15		5	20	9							0								0	20	30-70
Seminars	13				0.4		1	1.4	6	0	0		0			0								0	1.4	10-30
Research	34	4	4	6	8	8	8	38	42	0	0	0	0	0	0	0								0	38	80-140
	65	4	4	6	23	8	14	59	57	0	0	0	0	0	0	0	0	0	0	0	0	0	0	0	59	180

Bibliography

[1] Beckhoff Automation GmbH, "Beckhoff information system, TwinCAT 2," 2013. Verl, Germany.

[2] M. Higashimori, K. Utsumi, and M. Kaneko, "Dexterous hyper plate inspired by pizza manipulation," in *IEEE International Conference on Robotics and Automation (ICRA)*, pp. 399–406, 2008.